

Electronic Supplementary Information (ESI)

Aza-boron-diquinomethene complexes bearing *N*-aryl chromophores:
synthesis, crystal structures, tunable photophysics, protonation effect
and their application for pH sensor

Xiaolin Zhu,^a Hai Huang,^a Rui Liu,^{*a} Xiaodong Jin,^a Yuhao Li,^b Danfeng Wang,^a Qiang Wang,^a Hongjun Zhu^{*a}

a Department of Applied Chemistry, College of Sciences, Nanjing Tech University,
Nanjing 211816, P. R. China.

b Department of Chemistry, Fudan University, Shanghai 200433, P. R. China.

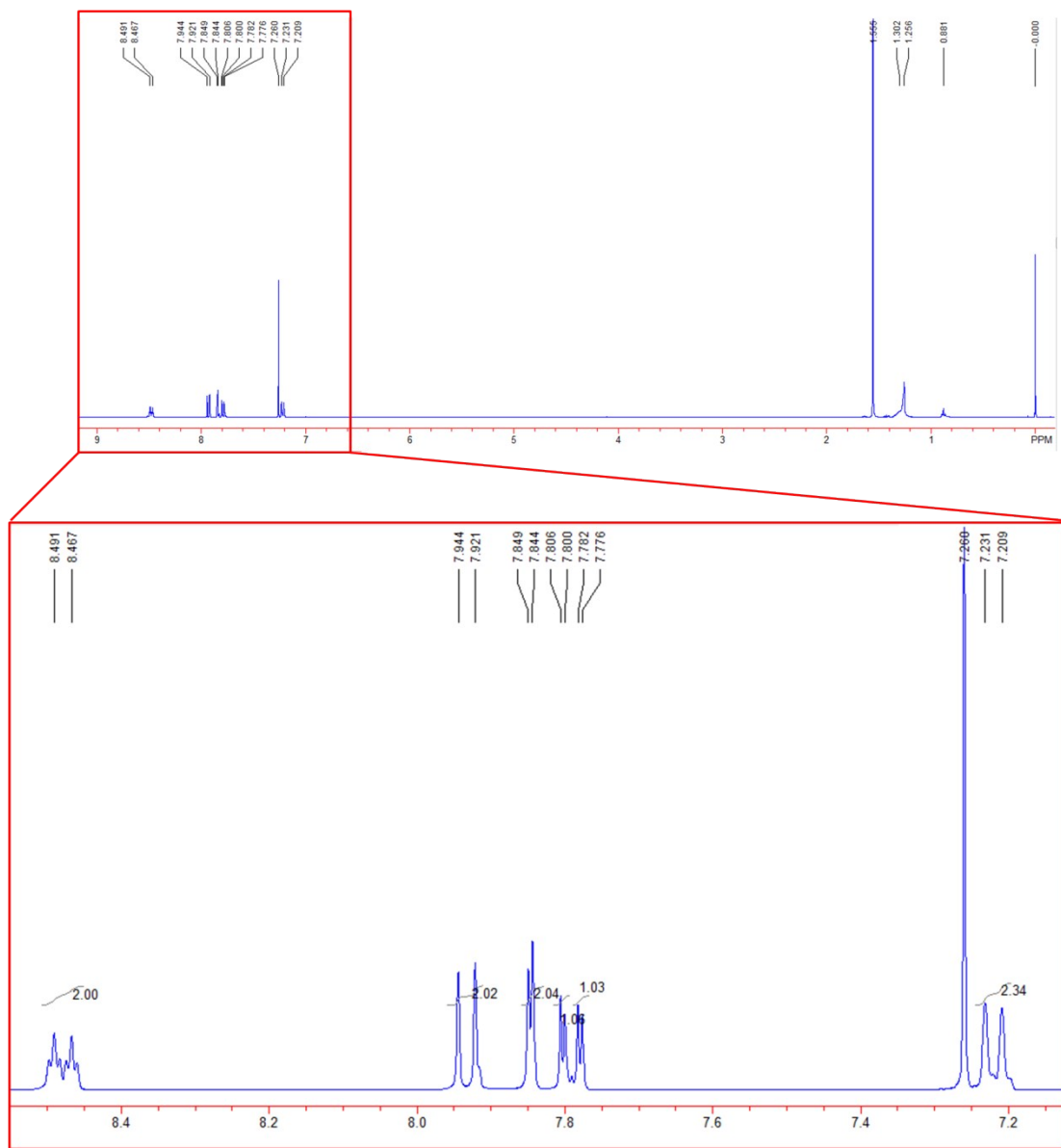


Figure S1. ¹H NMR spectrum of complex 1a.

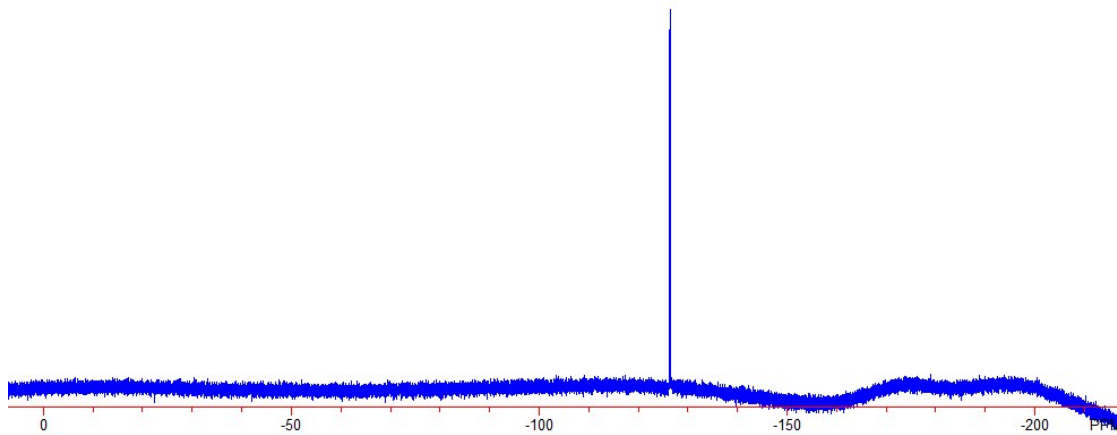


Figure S2. ¹⁹F NMR spectrum of complex 1a.

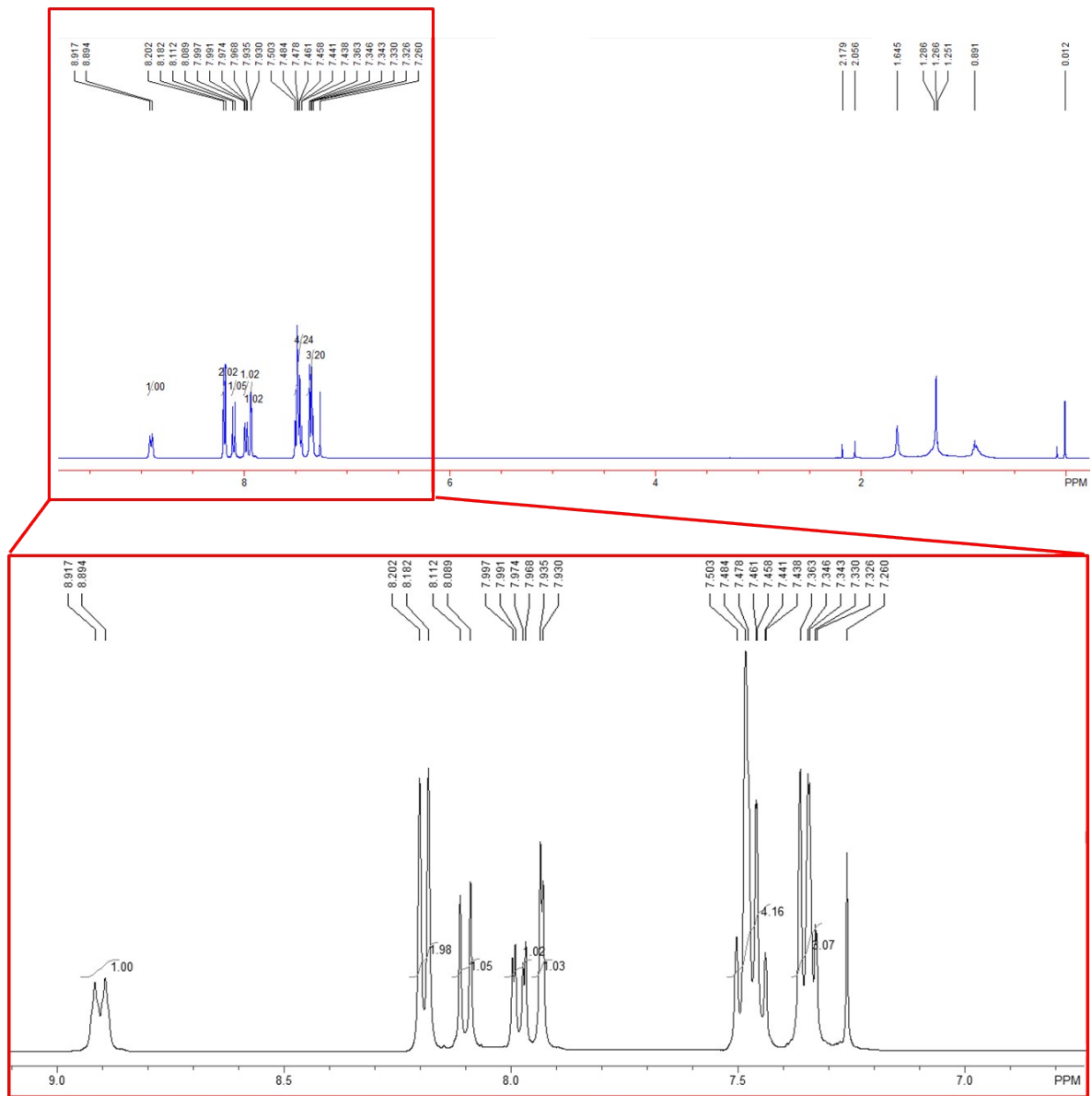


Figure S3. ¹H NMR spectrum of complex **1b**.

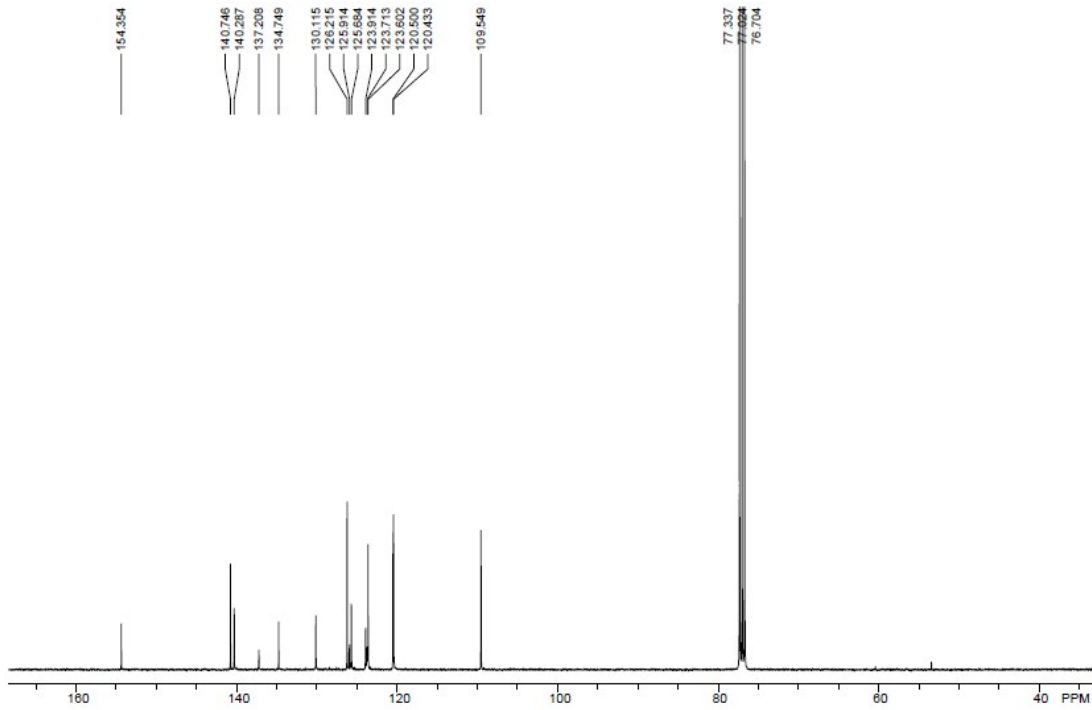


Figure S4. ¹³C NMR spectrum of complex **1b**.

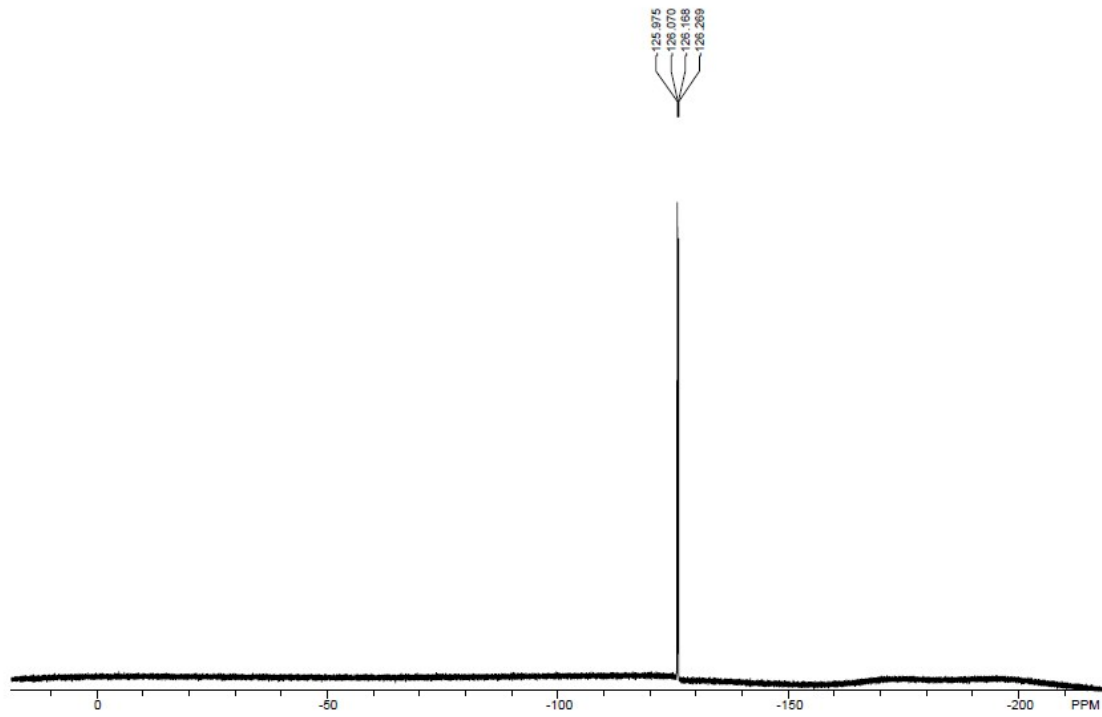


Figure S5. ¹⁹F NMR spectrum of complex **1b**.

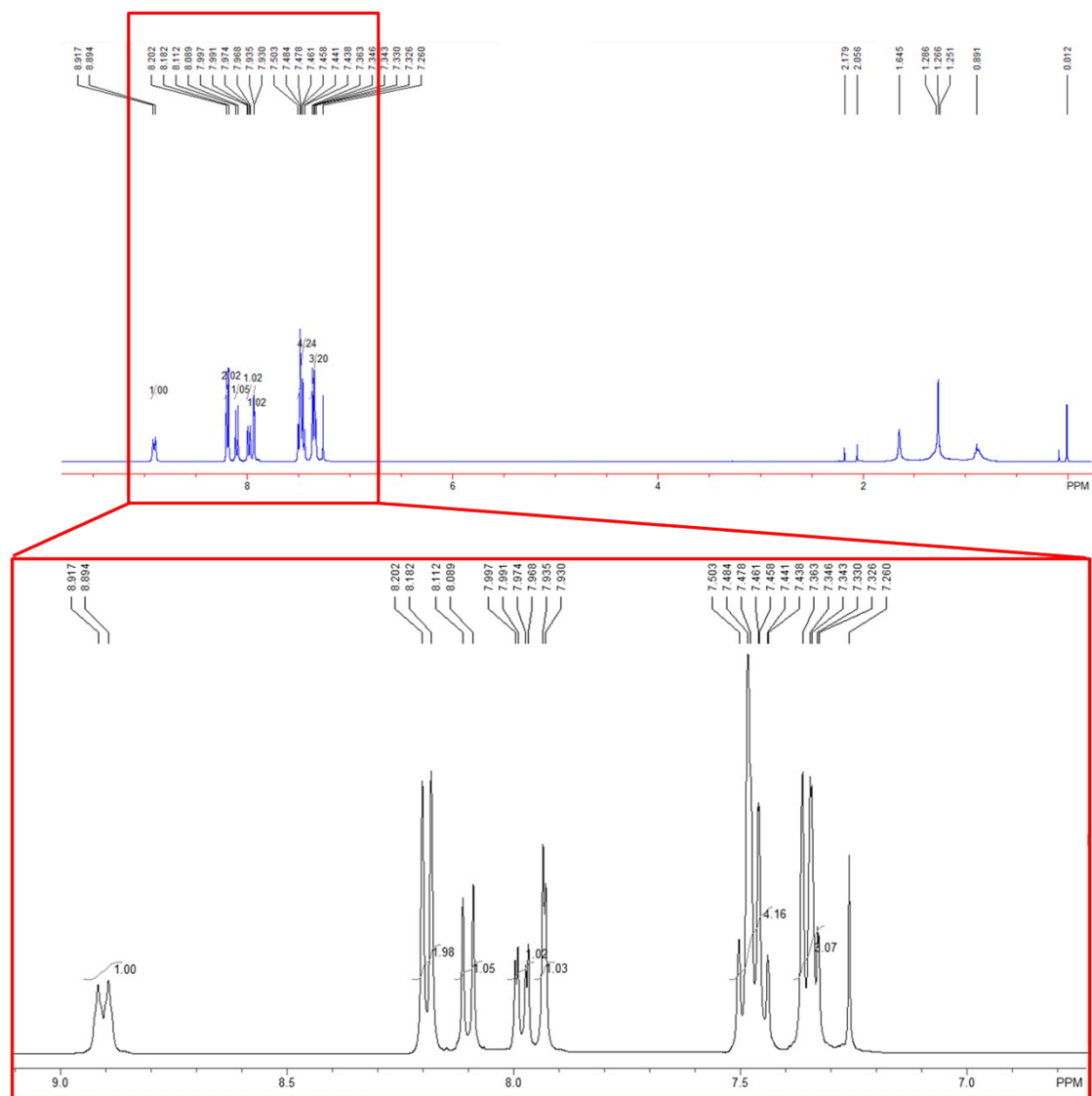


Figure S6. ¹H NMR spectrum of complex **1c**.

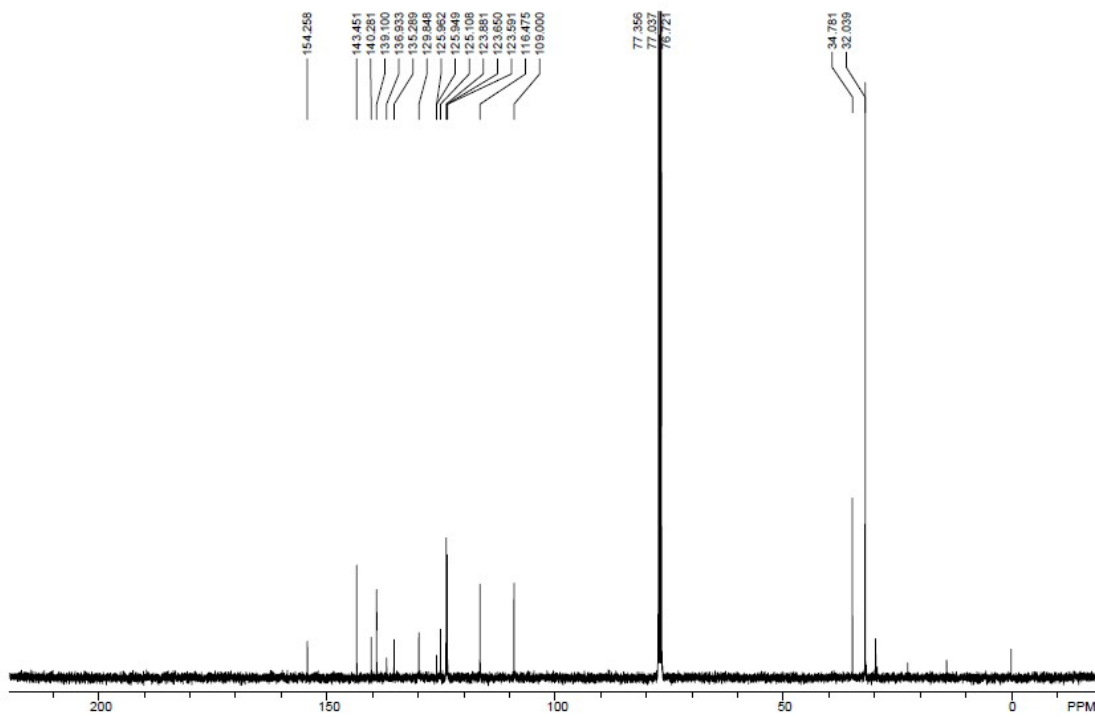


Figure S7. ¹³C NMR spectrum of complex **1c**.

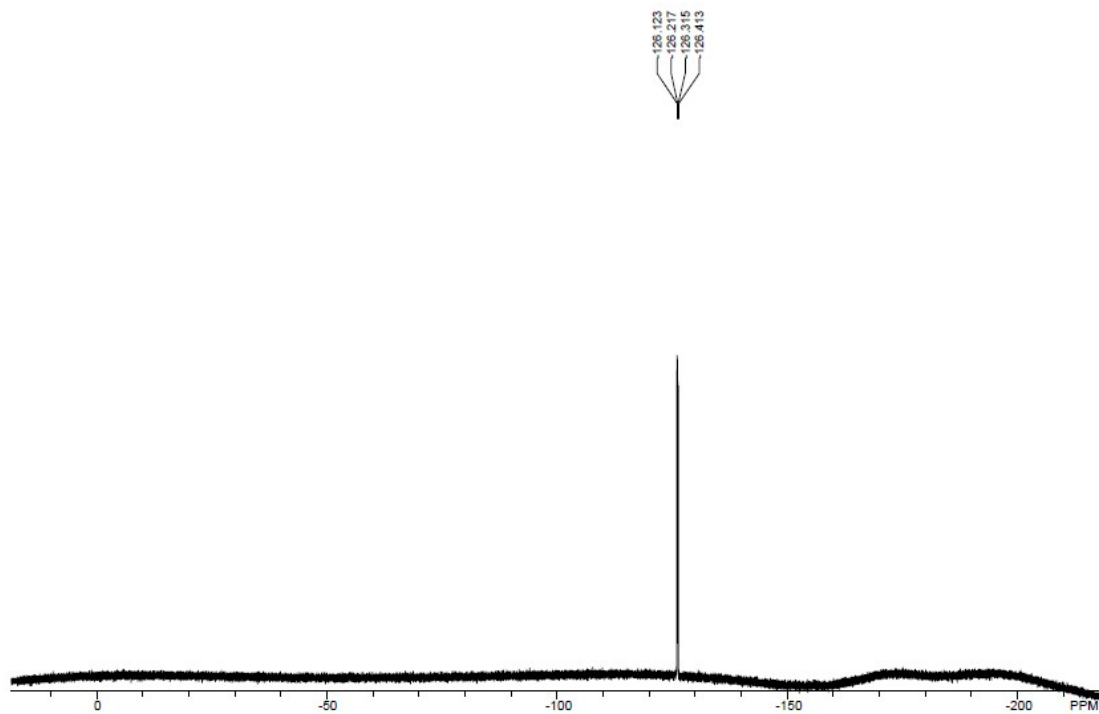


Figure S8. ¹⁹F NMR spectrum of complex **1c**.

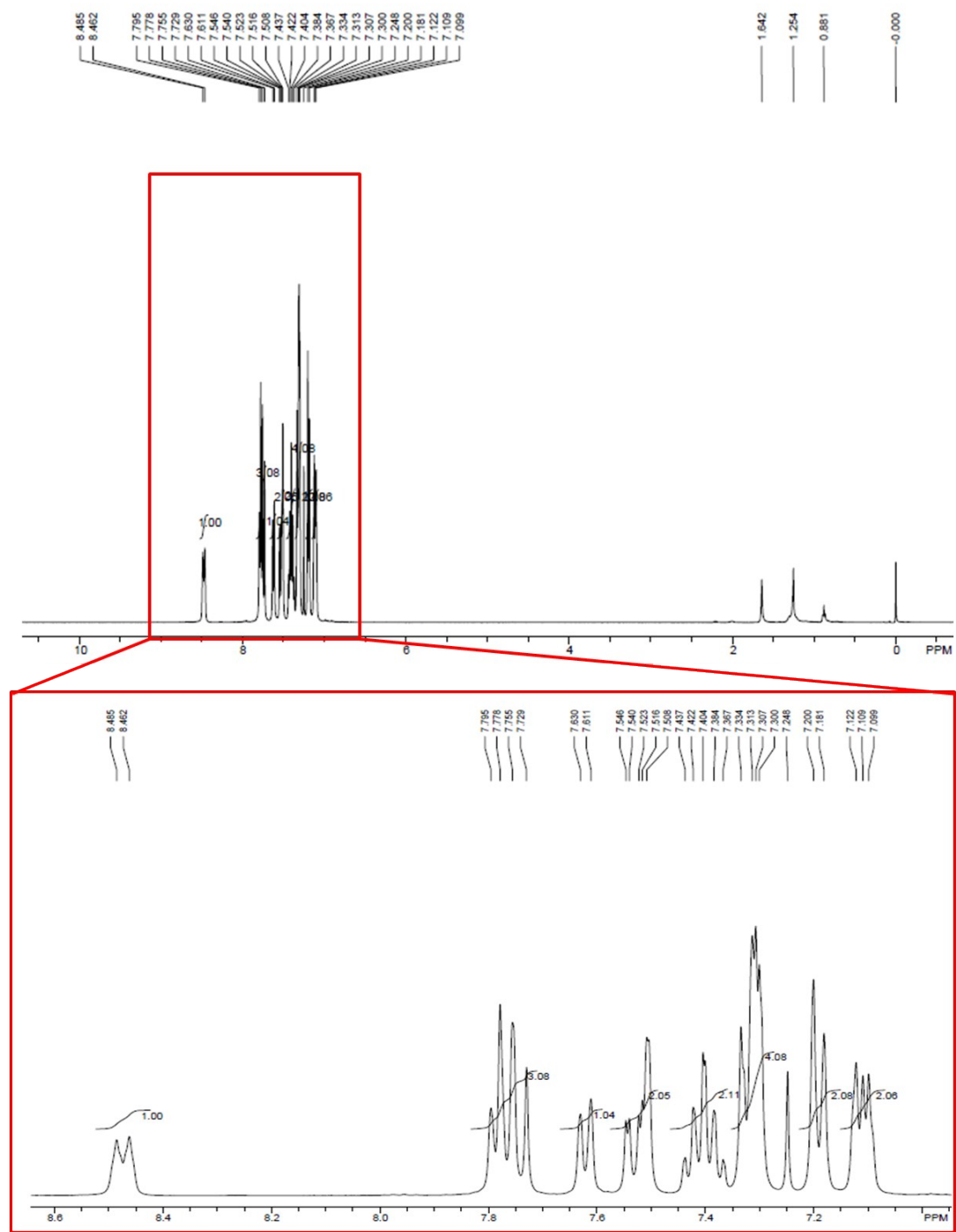


Figure S9. ^1H NMR spectrum of complex **1d**.

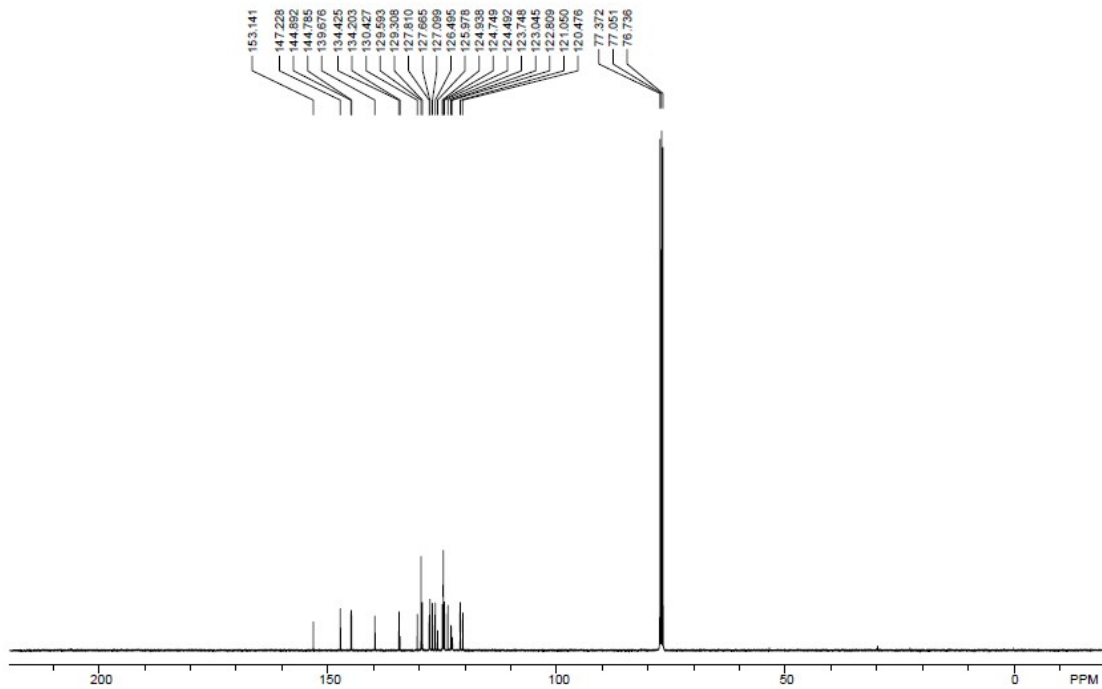


Figure S10. ¹³C NMR spectrum of complex 1d.

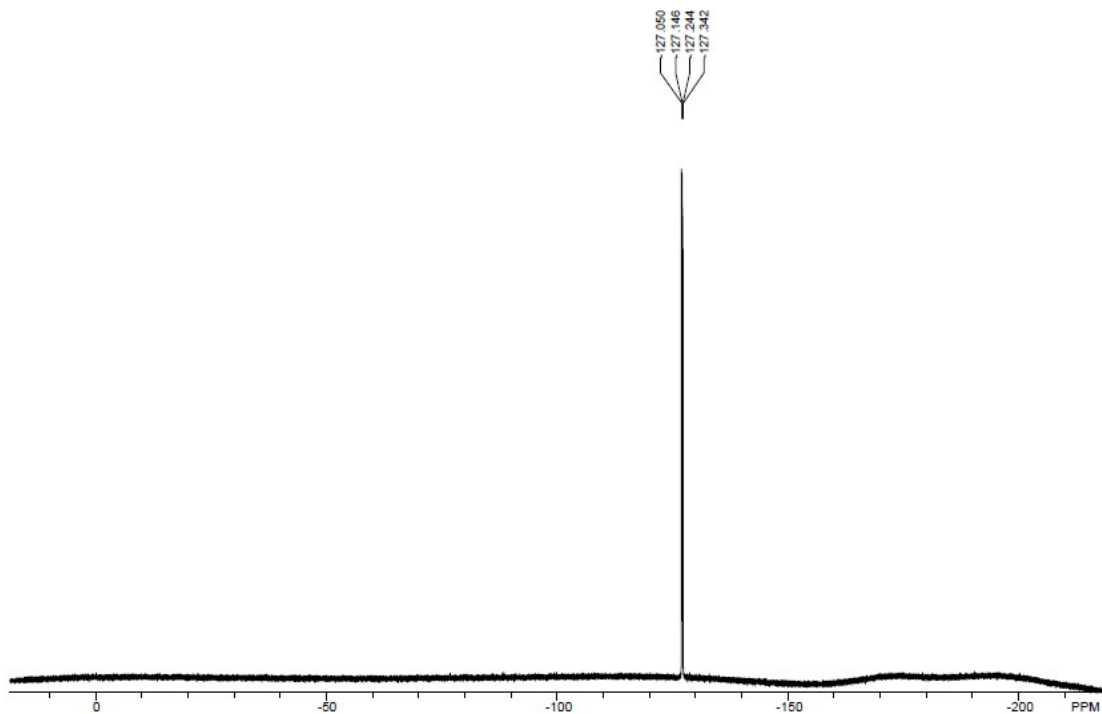
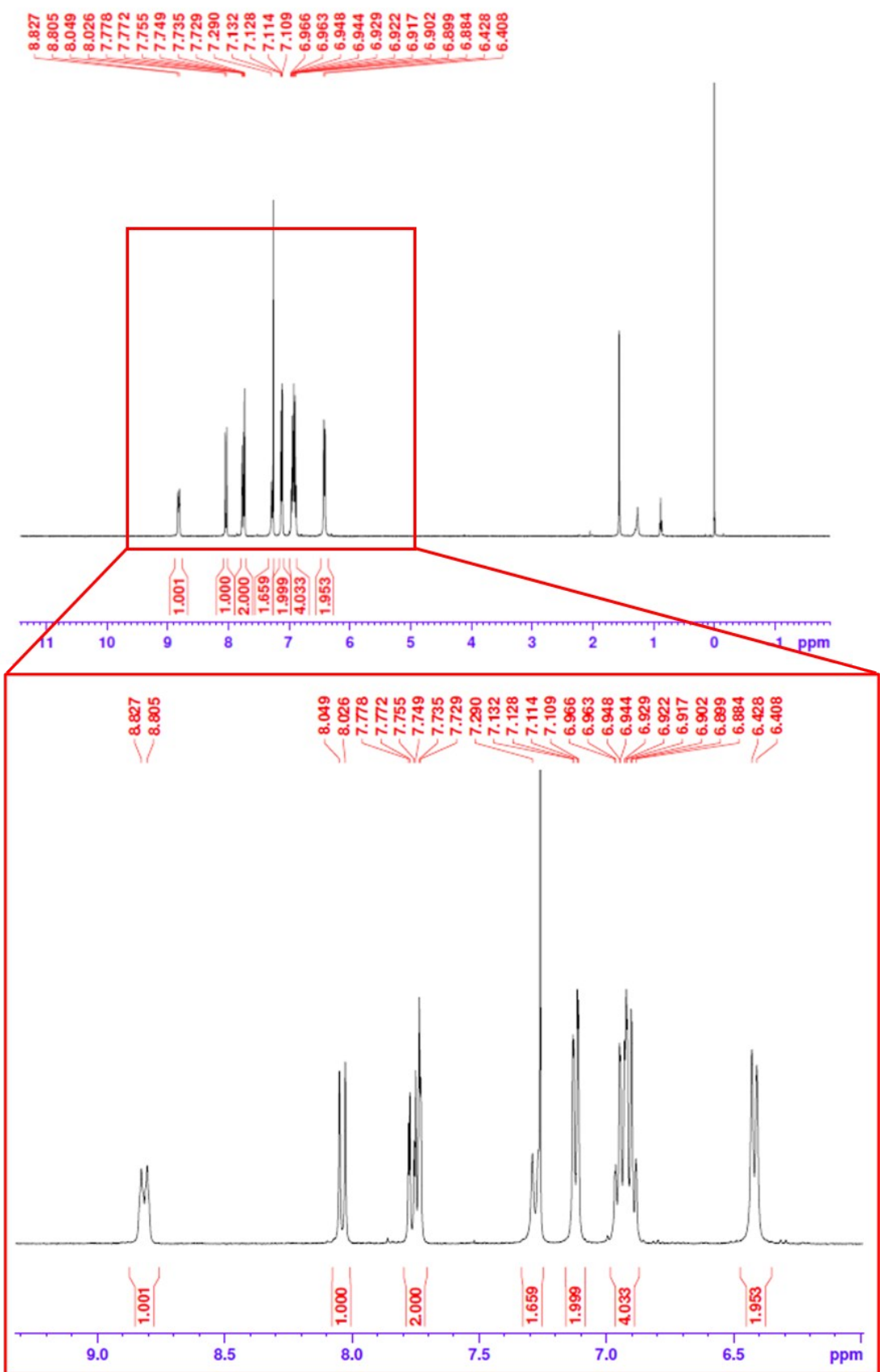


Figure S11. ¹⁹F NMR spectrum of complex 1d.



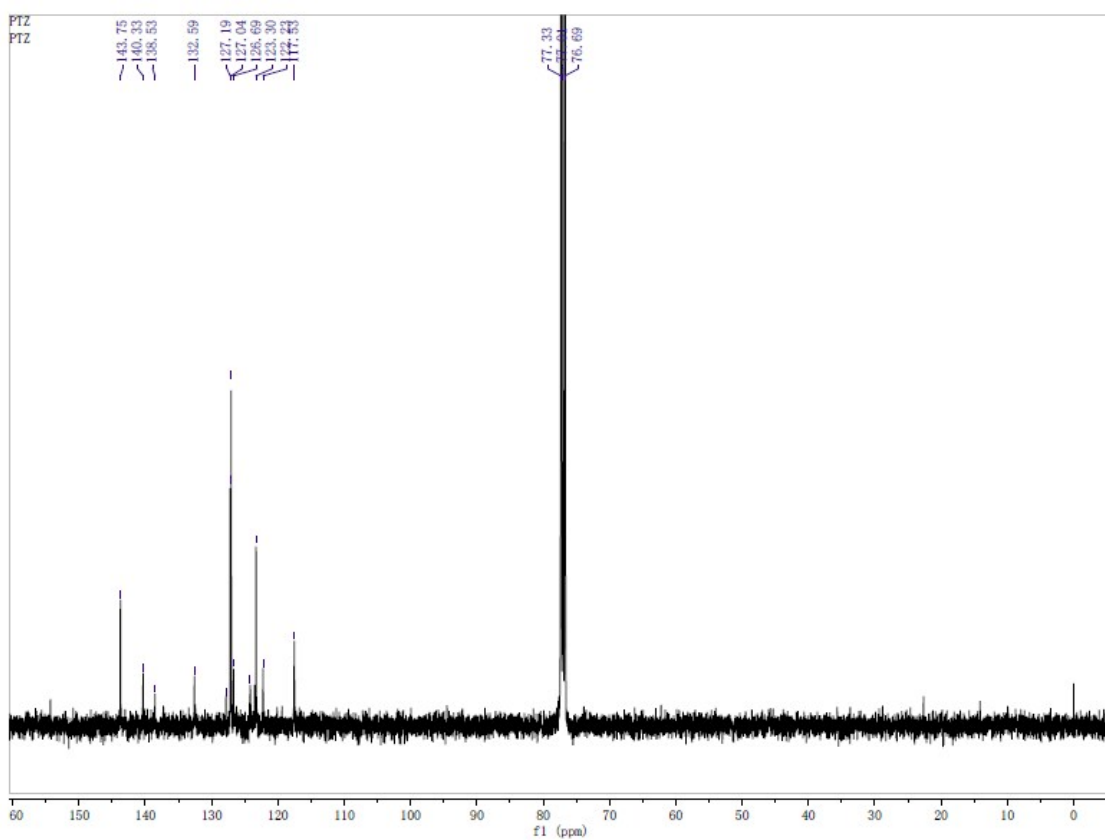


Figure S13. ^{13}C NMR spectrum of complex **1e**.

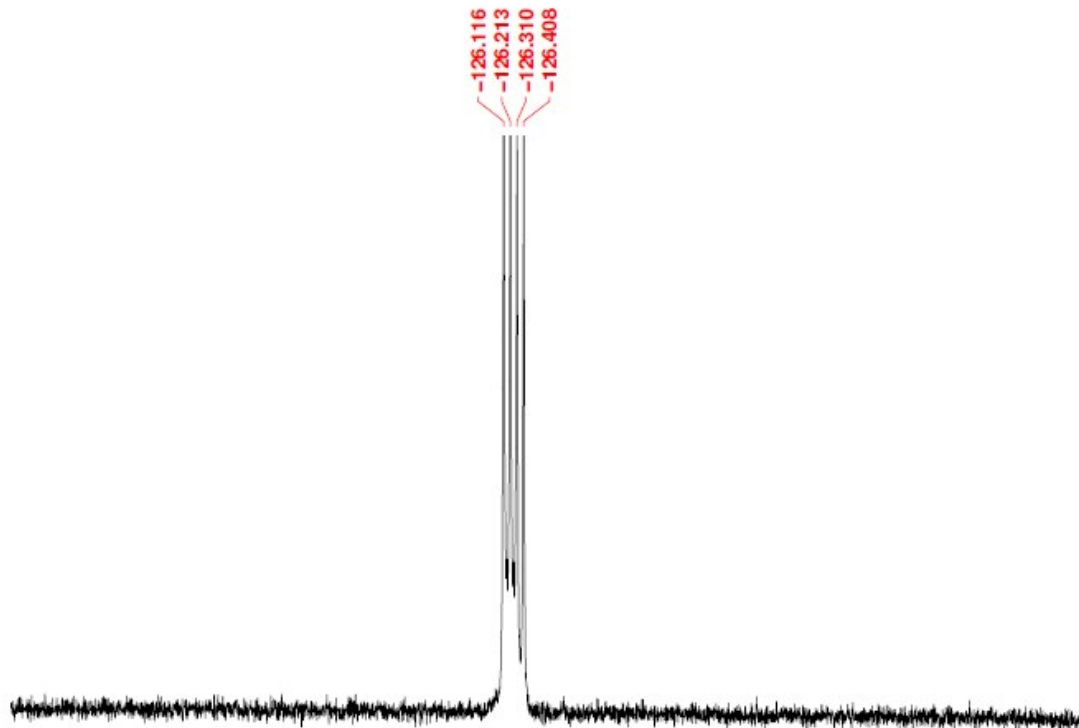


Figure S14. ^{19}F NMR spectrum of complex **1e**.

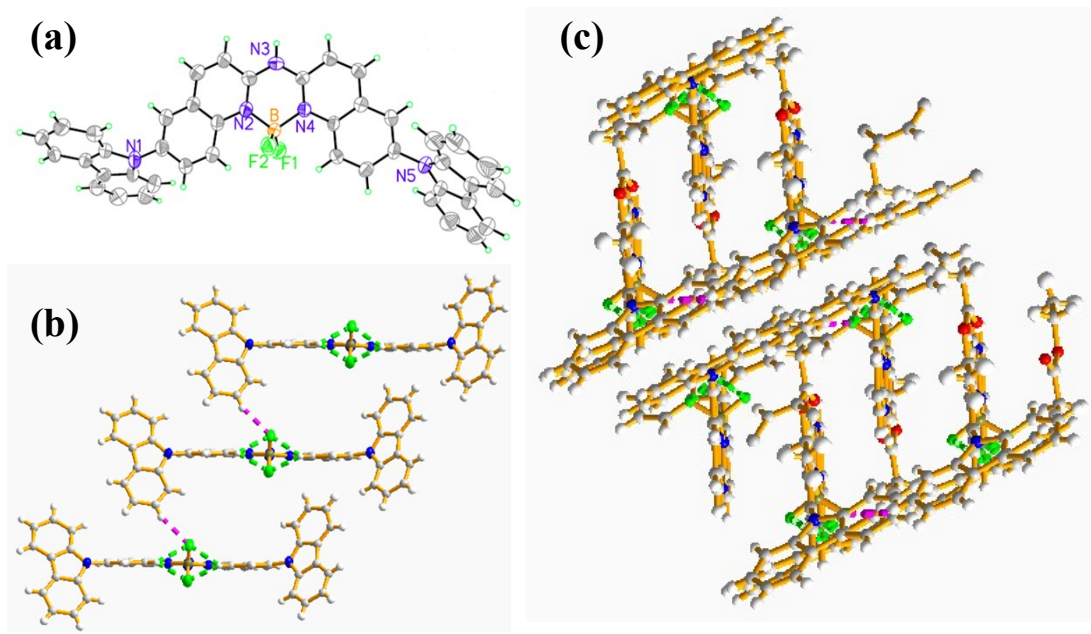


Figure S15. Molecular stacking in crystal for **1b**: green dotted lines: intramolecular C-H...F interaction (2.38-2.52 Å); purple dotted lines: intermolecular C-H...F interaction (3.73-3.79 Å).

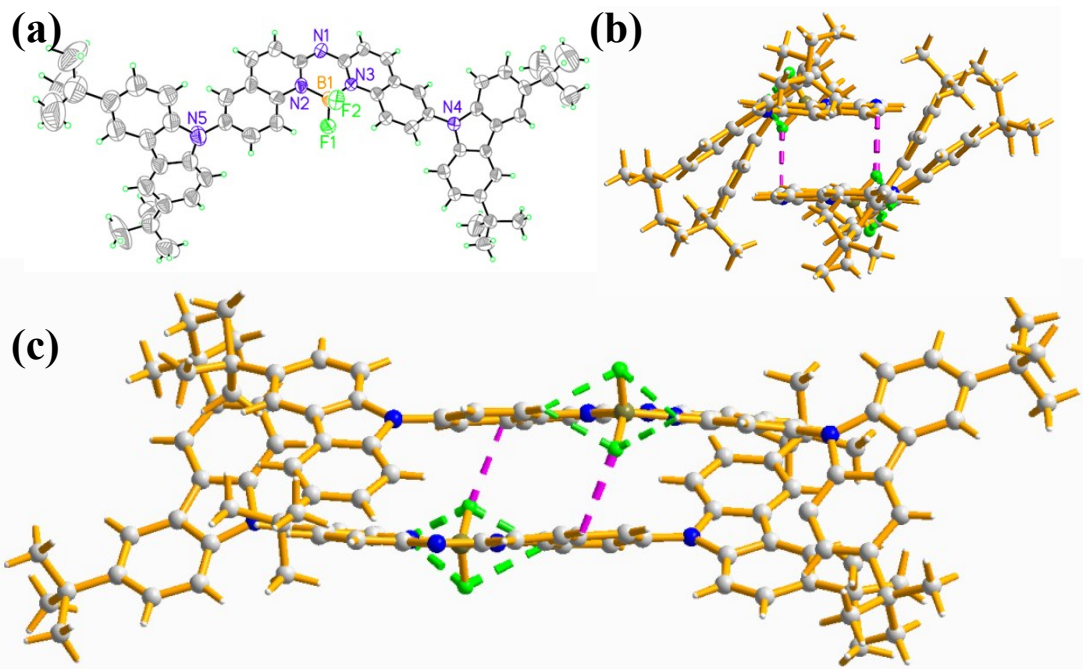


Figure S16. Molecular stacking in crystal for **1c**: green dotted lines: intramolecular C-H...F interaction (2.30-2.54 Å); purple dotted lines: intermolecular C-H...F interaction (3.71-3.73 Å).

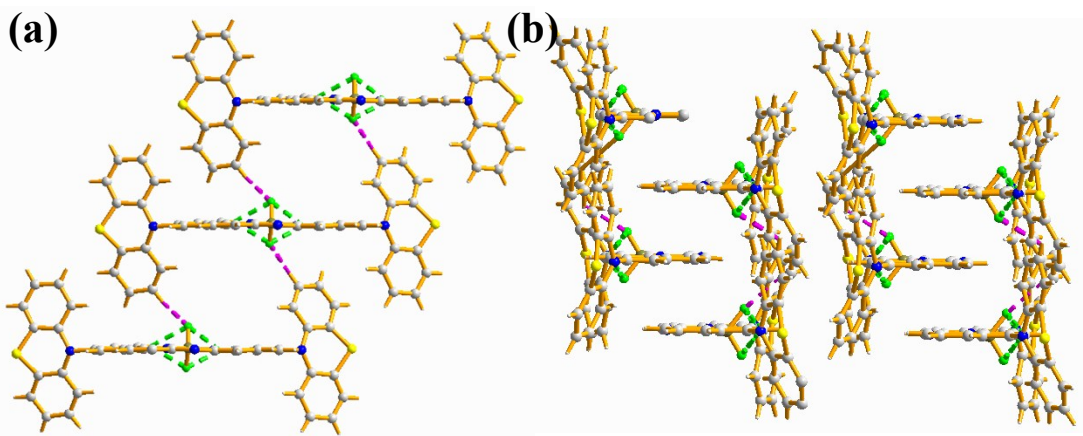


Figure S17. Molecular stacking in crystal for **1e**: green dotted line: C-H...F interaction (2.87-2.99 Å).

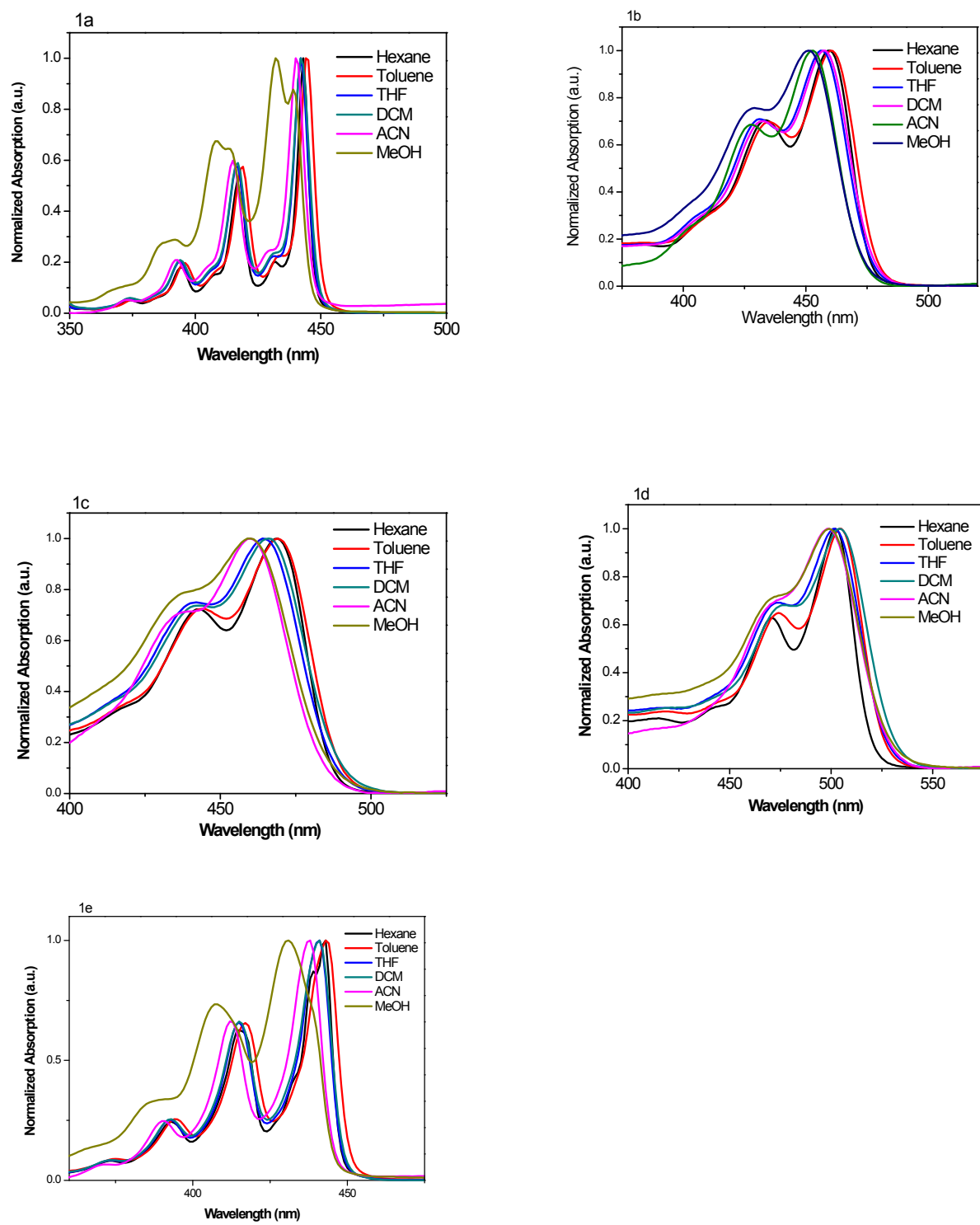


Fig. S18. Absorption spectra of **1a-1e** in different solvents (1×10^{-5} M).

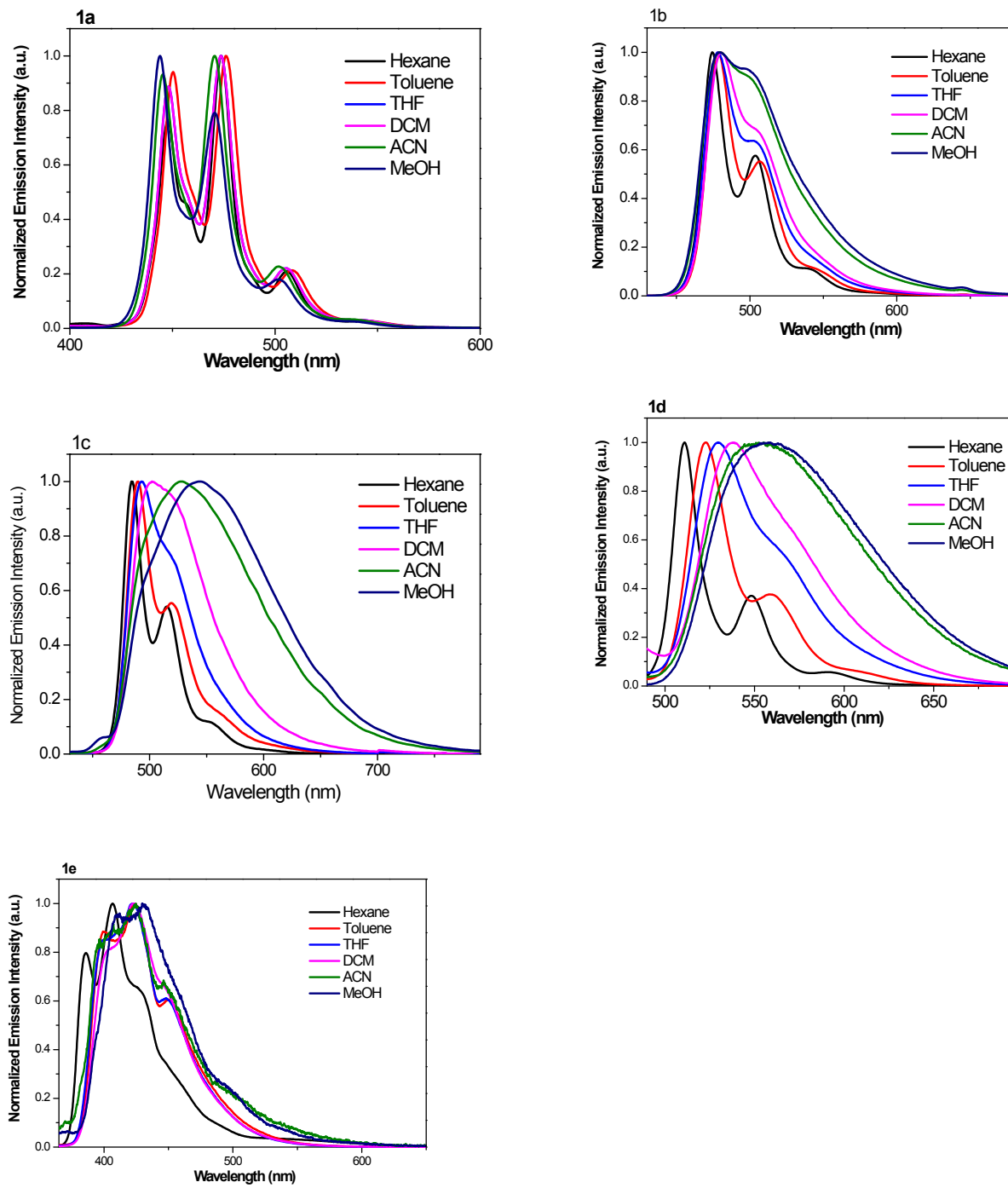


Fig. S19. Normalized emission spectra of **1a-1e** in different solvents (1×10^{-5} M).

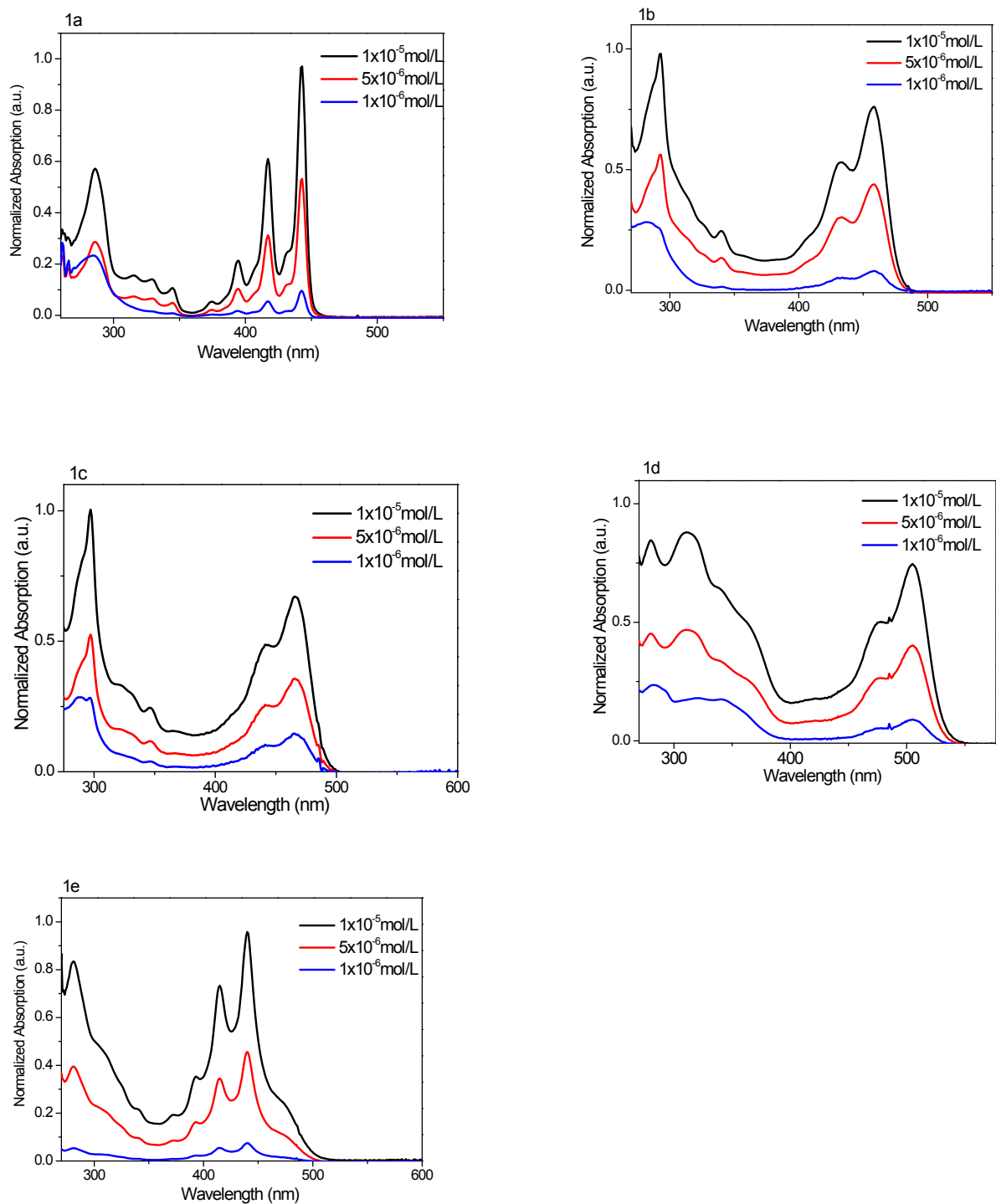


Fig. S20. Absorption spectra of **1a-1e** in CH_2Cl_2 of different concentrations (1×10^{-5} - $1 \times 10^{-6} \text{ M}$).

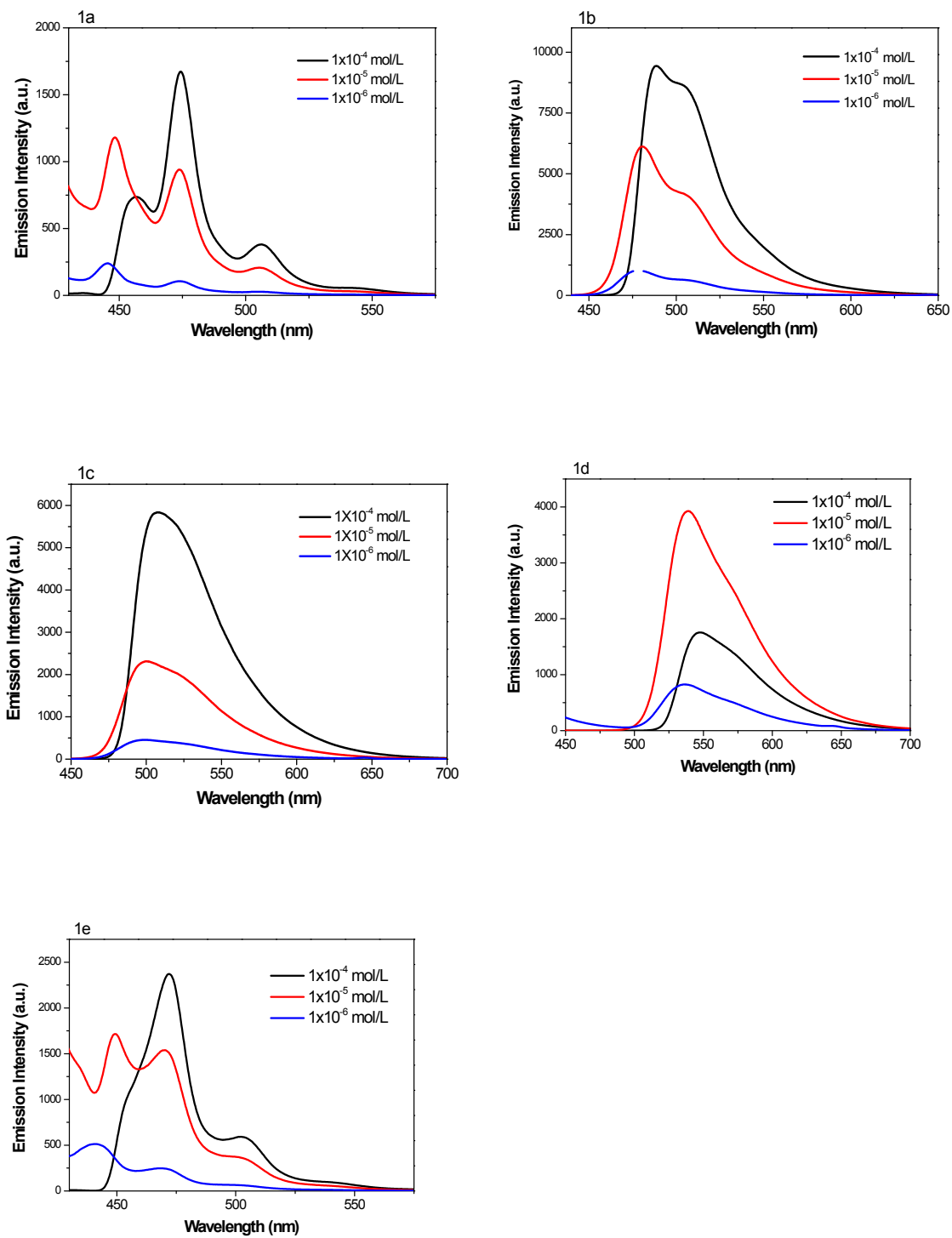


Fig. S21. Emission spectra of **1a-1e** in CH_2Cl_2 of different concentrations (1×10^{-6} - 1×10^{-4} M).

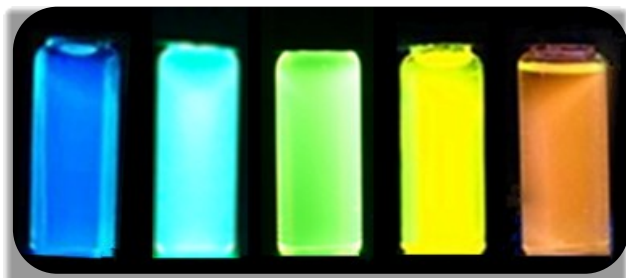


Fig. S22. Emission colours of **1a-1d** in CH_2Cl_2 of concentrations (1×10^{-5} M), **1e** in THF-H₂O (1/9, 1×10^{-5} M).

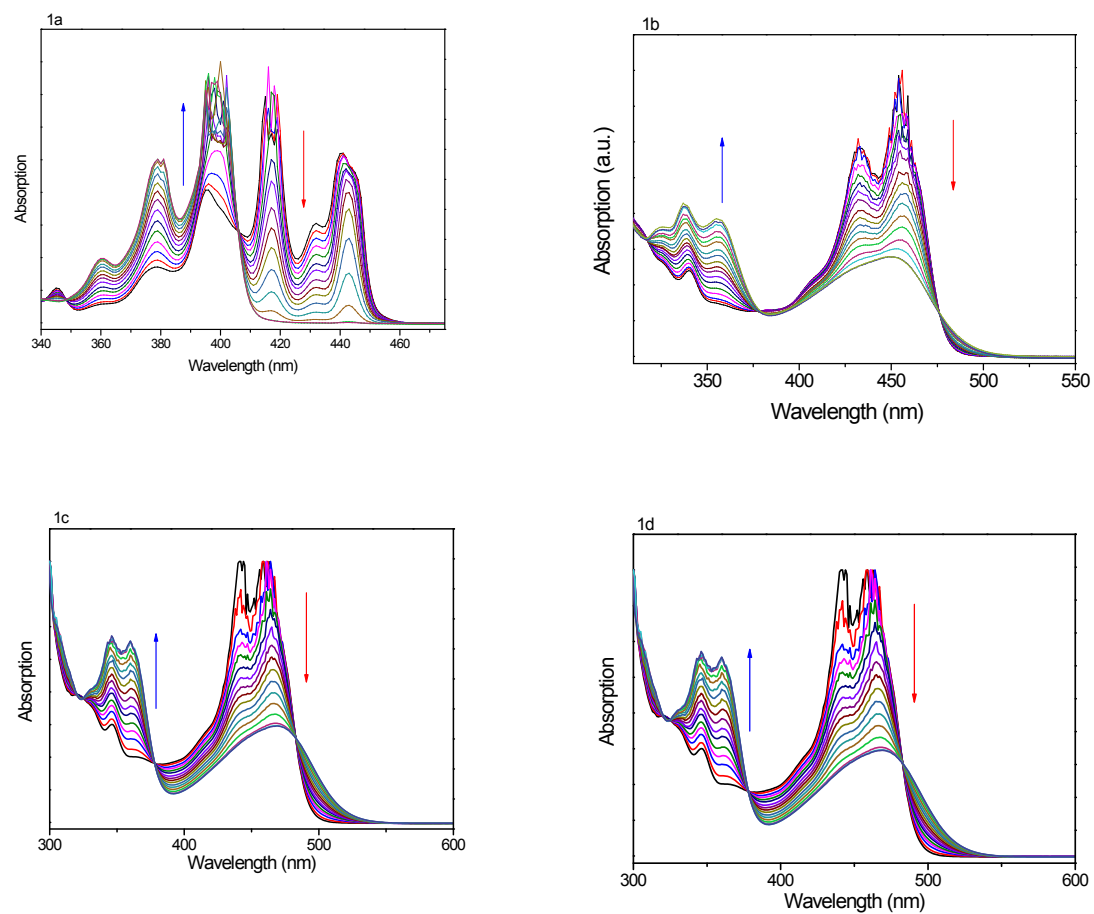


Fig. S23. Absorption spectra of **1a-1d** in CH_2Cl_2 with addition of p-TsOH/ CH_3CN solution.

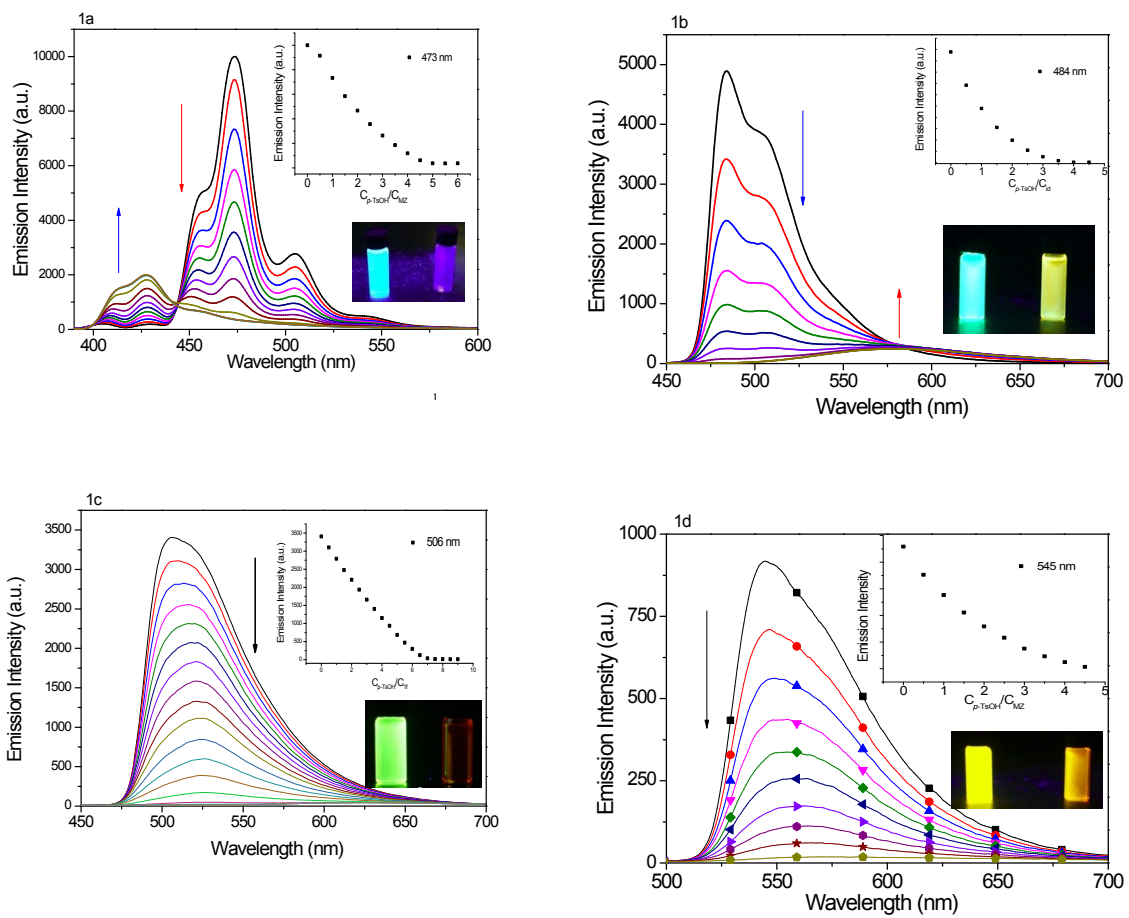


Fig. S24. Emission spectra of **1a-1d** in CH_2Cl_2 with addition of p-TsOH/CH₃CN solution.

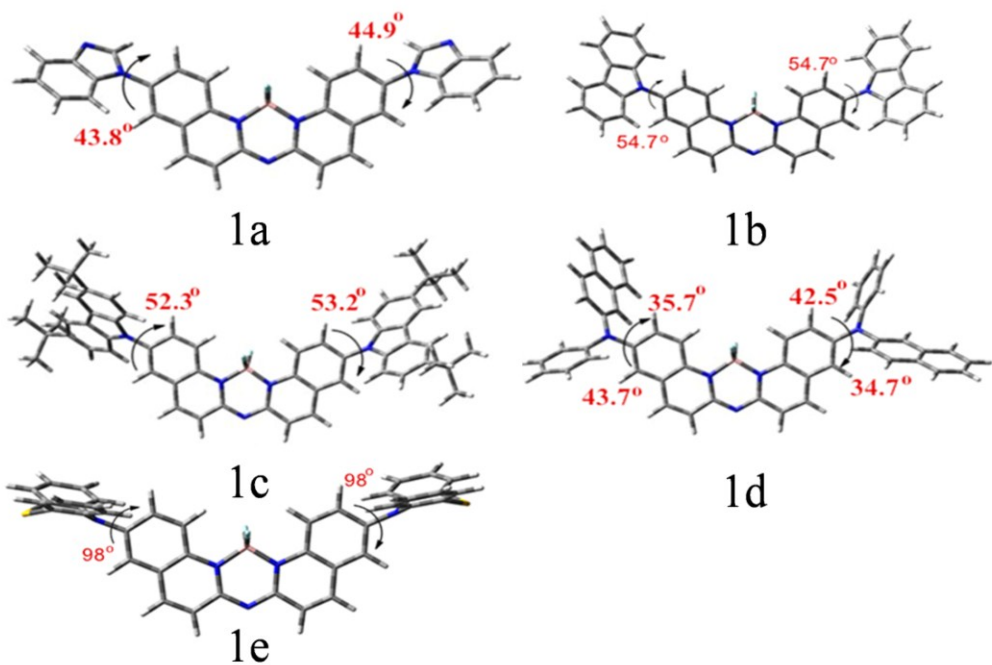


Fig. S25. The dihedral angles of the rings between nitrogen heterocyclic rings and cores according to the ground-state optimized structure of **1a-1e** in gas state.

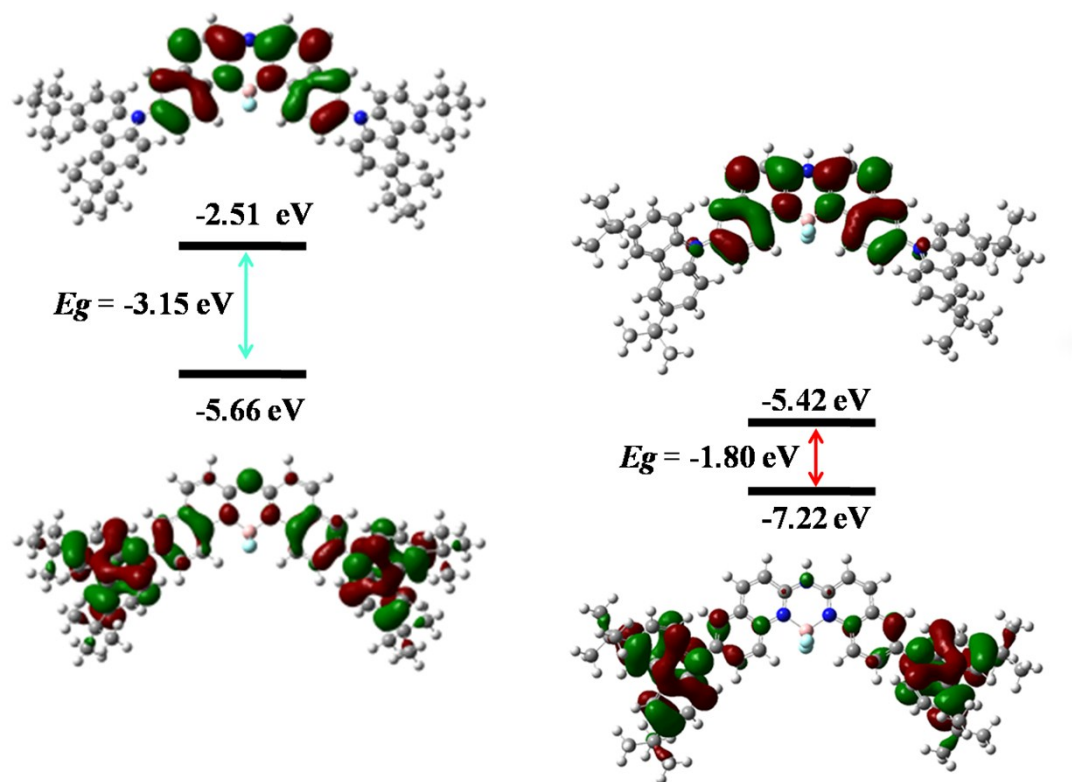
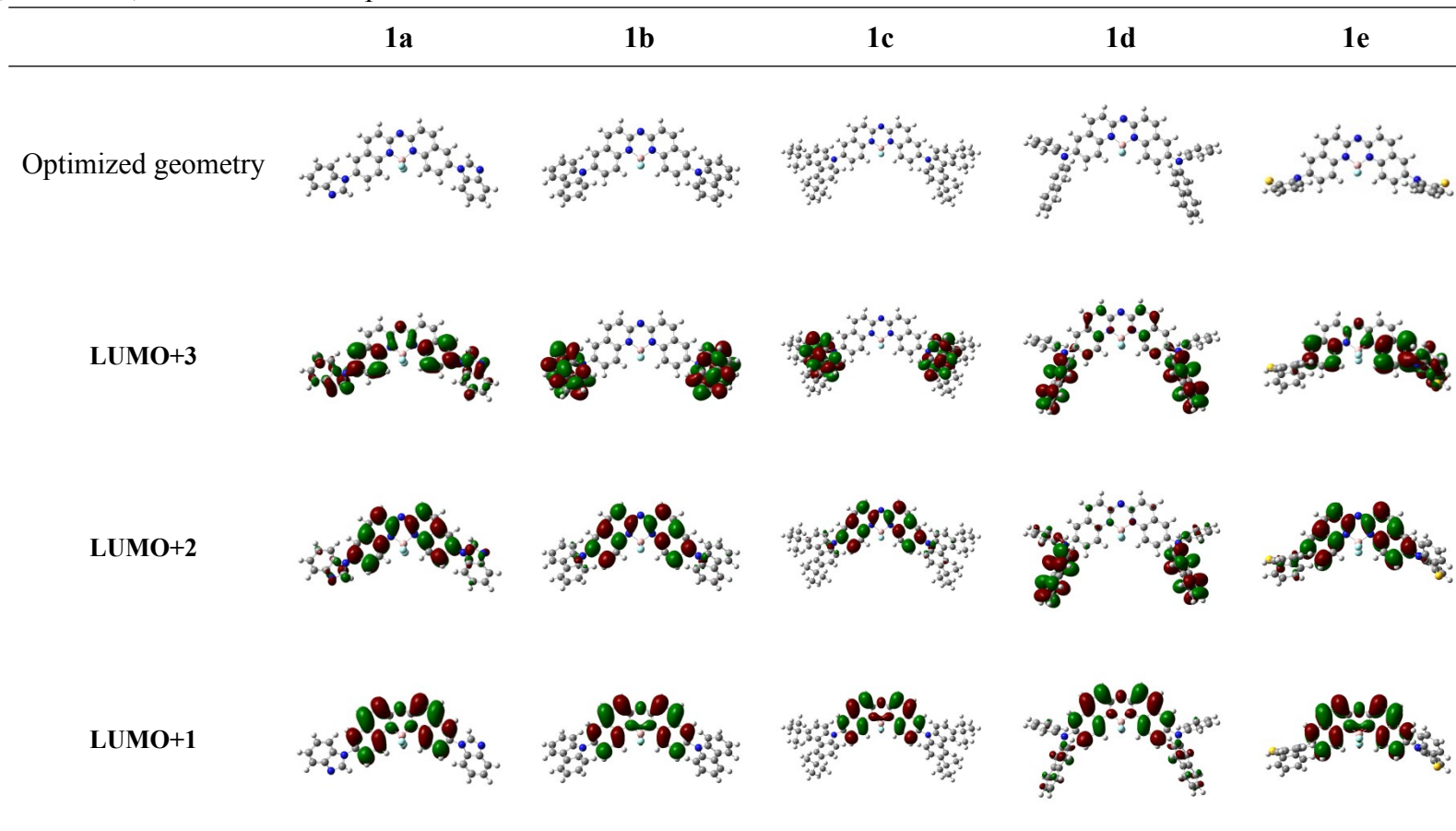


Fig. S26. Molecular orbital amplitude plots of (upper) LUMO and (lower) HOMO of **1c** and **1c-H⁺** in gas state.

Table S1. Contour plots of the occupied molecular orbital HOMO, HOMO-1, HOMO-2, HOMO-3 and unoccupied molecular orbital LUMO, LUMO+1, LUMO+2, LUMO+3 for complexes **1a-1e**.



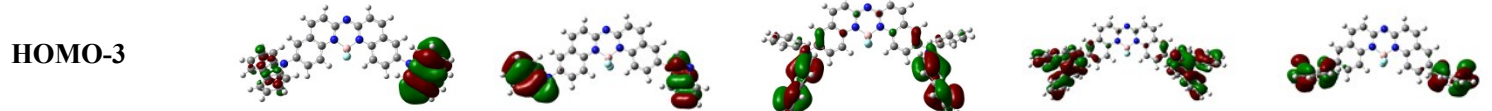
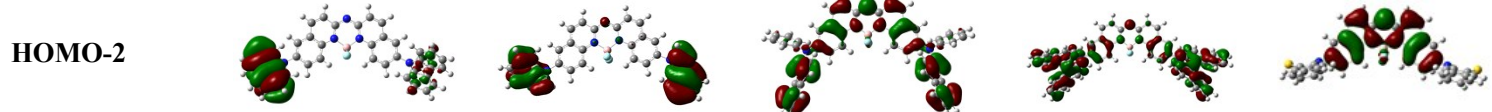
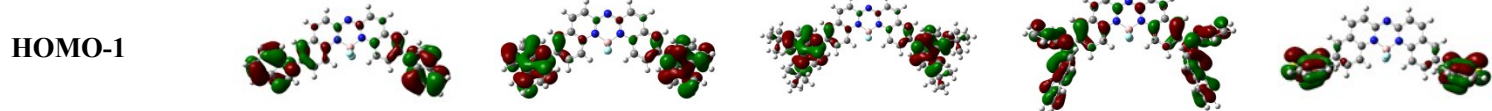
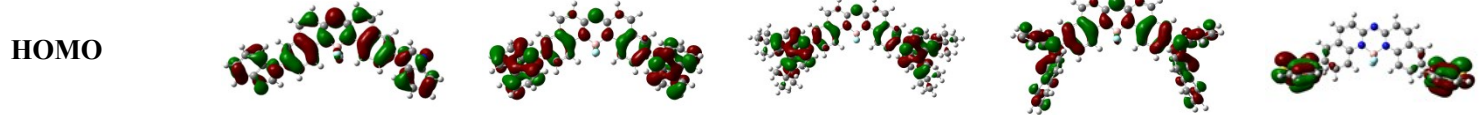
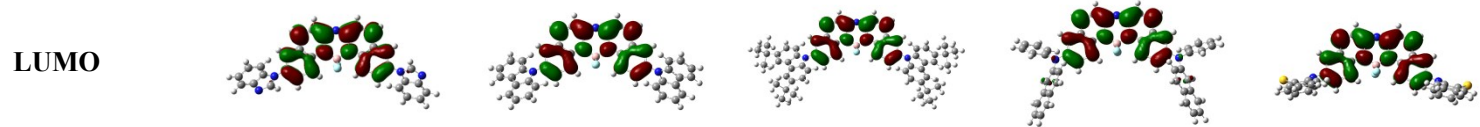


Table S2. DFT-derived molecular orbital energies (eV) of **1a-1e**

	1a	1b	1c	1d	1e
LUMO+	-	-	-0.98313	-	-
3	0.87374	1.08272		1.26966	0.61226
LUMO+	-	-	-1.10014	-	-
2	1.16245	1.19265		1.27184	1.05908
LUMO+	-	-	-1.77415	-	-
1	1.84300	1.85905		1.57089	1.70073
LUMO	-	-	-2.50613	-	-
	2.56926	2.59511		2.25089	2.43217
HOMO	-	-	-5.65553	-	-
	5.90288	5.88519		5.34913	5.06353
HOMO-	-	-	-5.76465	-	-
1	6.06179	6.01580		5.57907	5.06381
HOMO-	-	-	-	-	-
2	6.40682	6.36329	6.238121	6.28029	5.97322
HOMO-	-	-	-6.23812	-	-
3	-6.5415	6.36329		6.51213	6.10710

Table S3. Summary of the molecular interactions in the crystals

Crystal	Orientation of Interaction		d (Å)	A (Å)
1b-C₄H₈O₂-0.5C₄H₆	I	C-H...π	3.734(2)	113(1)
	II	C-H...π	3.794(2)	115(1)
	III	C-H...F	2.942(1)	118(1)
	IV	C-H...F	2.982(1)	113(1)
	V	C-H...F	2.963(1)	116(1)
	VI	C-H...F	3.044(1)	116(1)
	VII	C-H...F	3.372(1)	155(1)
1c	I	C-H...π	3.717(2)	115(1)
	II	C-H...π	3.731(2)	117(1)
	III	C-H...F	2.870(2)	119(1)
	IV	C-H...F	2.900(2)	115(1)
	V	C-H...F	3.033(2)	117(1)
	VI	C-H...F	3.060(2)	115(1)
1e	I	C-H...π	3.264(2)	159(1)

II	C-H... π	3.162(2)	125(1)
III	C-H... π	3.053(2)	160(1)
IV	C-H... π	2.930(2)	141(1)
V	C-H...F	2.758(1)	149(1)
VI	C-H...F	2.735(1)	142(1)
VII	C-H...F	2.908(1)	119(1)
VIII	C-H...F	2.982(1)	112(1)
IX	C-H...F	2.872(1)	115(1)
X	C-H...F	2.986(1)	118(1)
XI	C-S...H	3.031(1)	159(1)
XII	C-S...H	3.054(1)	157(1)

Table S4. Crystallographic data of three crystals

	1b-C₄H₈O₂-0.5C₄H₆	1c	1e
Empirical formula	C ₄₈ H ₃₈ BF ₂ N ₅ O ₂	C ₅₈ H ₅₈ BF ₂ N ₅	C ₄₂ H ₂₆ BF ₂ N ₅ S ₂
Formula wt	765.64	873.90	713.61
T,K	293	296	293
Crystal system	Triclinic	Monoclinic	Triclinic
Space group	P-1	P2 ₁ /c	P-1
a, Å	9.0720(18)	22.4457(17)	8.2448(13)
b, Å	15.181(3)	11.3035(7)	13.187(2)
c, Å	16.186(3)	20.0181(14)	19.061(3)
α, deg	65.63(3)	90.00	100.053 (1)
β, deg	86.22(3)	92.623(5)	95.703 (1)
γ, deg	77.79(3)	90.00	95.546 (1)
V, Å ³	1984.0(9)	5073.6(6)	2016.7(6)
Z	2	4	2
d(cald), Mg/m ³	1.282	1.144	1.175
absorption coefficient, mm ⁻¹	0.086	0.564	0.176
θ range, deg	1.4-25.4	3.94-66.09	3.43-65.10
no. of reflnscollected	7776	8338	6645
no. of uniquerefns	7277	5352	2740
R(int)	0.0361	0.0535	0.0727
goodness-of-fit on F ²	1.009	1.191	0.927
RI[$I > 2\sigma(I)$]	0.0767	0.1316	0.0952
wR2 [$I > 2\sigma(I)$]	0.1565	0.2674	0.2014
RI(all data)	0.1575	0.1661	0.1690
wR2(all data)	0.1875	0.2800	0.2340

Table S5. Structural parameters for **1c** and **1c-H⁺** calculated using Gaussian 09,

B3LYP/6-31-G* basis set		
Structural parameter	1c	1c-H⁺
Bond length (Å)		
C1-N4	1.4156	1.3961
C37-N5	1.4156	1.3961
Dihedral angle (°)		
C1-N4-C21-C22	52.3	43.0
C39-N5-C37-C38	53.2	43.0